BIOCHEMISTRY
including biophysical chemistry & molecular biology
Article

Biochemistry **2009,** *48,* 6259–6267 6259
DOI: 10.1021/bi802332j

Mechanistic Investigations of Human Reticulocyte 15- and Platelet 12-Lipoxygenases with Arachidonic Acid†

Aaron T. Wecksler,‡ Cyril Jacquot,§ Wilfred A. van der Donk,*,§ and Theodore R. Holman*,‡

‡*Chemistry and Biochemistry Department, University of California, Santa Cruz, California 95064, and* §*Department of Chemistry, University of Illinois, 600 South Mathews Avenue, Urbana, Illinois 61801*

Received December 21, 2008; Revised Manuscript Received May 22, 2009

ABSTRACT: Human reticulocyte 15-lipoxygenase-1 (15-hLO-1) and human platelet 12-lipoxygenase (12-hLO) have been implicated in a number of diseases, with differences in their relative activity potentially playing a central role. In this work, we characterize the catalytic mechanism of these two enzymes with arachidonic acid (AA) as the substrate. Using variable-temperature kinetic isotope effects (KIE) and solvent isotope effects (SIE), we demonstrate that both k_{cat}/K_M and k_{cat} for 15-hLO-1 and 12-hLO involve multiple rate-limiting steps that include a solvent-dependent step and hydrogen atom abstraction. A relatively low k_{cat}/K_M KIE of 8 was determined for 15-hLO-1, which increases to 18 upon the addition of the allosteric effector molecule, 12-hydroxyeicosatetraenoic acid (12-HETE), indicating a tunneling mechanism. Furthermore, the addition of 12-HETE lowers the observed k_{cat}/K_M SIE from 2.2 to 1.4, indicating that the rate-limiting contribution from a solvent sensitive step in the reaction mechanism of 15-hLO-1 has decreased, with a concomitant increase in the C−H bond abstraction contribution. Finally, the allosteric binding of 12-HETE to 15-hLO-1 decreases the $K_M[O_2]$ for AA to 15 μM but increases the $K_M[O_2]$ for linoleic acid (LA) to 22 μM, such that the $k_{cat}/K_M[O_2]$ values become similar for both substrates ($\sim$0.3 s^{-1} μM^{-1}). Considering that the oxygen concentration in cancerous tissue can be less than 5 μM, this result may have cellular implications with respect to the substrate specificity of 15-hLO-1.

In the human cell, hydroperoxidation of polyunsaturated fatty acids using molecular oxygen is accomplished by the human lipoxygenase (hLO) isozyme family (Scheme 1) (*1*). 5-hLO, 12-hLO,[1] and 15-hLO are the three main lipoxygenases and are named according to their positional specificity on arachidonic acid (AA), producing their respective hydroperoxyeicosatetraenoic acid (HPETE) products. The LO products are responsible for the human inflammatory response (*2*), and they are also implicated in a variety of human diseases. 5-hLO is involved in asthma (*3*) and cancer (*4*, *5*), 12-hLO in psoriasis (*6*) and cancer (*5*, *7*, *8*), and 15-hLO in atherosclerosis (*9*) and cancer (*5*, *10*).

Recently, the substrate specificity of the 15-hLO isozymes has been suggested to play a role in prostate cancer since their respective products have different cellular responses (*11*−*13*). Reticulocyte 15-hLO-1 and epithelial 15-hLO-2 react with both linoleic acid (LA) and AA, although 15-hLO-1 reacts preferentially with LA while 15-hLO-2 reacts preferentially with AA (*14*−*16*). The substrate specificity of both 15-hLO-1 and 15-hLO-2, however, can be affected by product binding to their allosteric sites, suggesting an autoregulatory mechanism (*14*). In contrast, 5-hLO and platelet 12-hLO (12-hLO) are more substrate selective and react only with AA. For the sake of comparison, soybean lipoxygenase-1 (sLO-1), a plant homologue and model enzyme for 15-hLO-1, also reacts preferentially with AA over LA (*14*, *17*), even though AA is not a native substrate in soybeans.

With regard to the general mechanism of lipoxygenase, the as-isolated enzyme is in the inactive Fe(II)−OH_2 form and is activated to the Fe(III)−OH form by the hydroperoxide product, resulting in an observable kinetic lag phase (Scheme 1). A hydrogen atom is irreversibly abstracted from the 1,4-diene, forming a Fe(II)−OH_2/pentadienyl radical intermediate (i.e., the reductive half-reaction). Oxygen attacks the pentadienyl radical intermediate, forming a hydroperoxide radical, which is reduced by the Fe(II)−OH_2 species to form the product, leaving the active Fe(III)−OH species (i.e., the oxidative half-reaction) (*1*). This general mechanism is based on extensive studies

†This work was supported by the National Institutes of Health [S10-RR20939 (MS Equipment Grant), GM44911 (W.A.v.d.D.), and GM56062 (T.R.H.)], an American Heart Association predoctoral fellowship (0615604Z to C.J.), and the California Institute for Quantitative Biosciences (MS Facility grant).

*To whom correspondence should be addressed. W.A.v.d.D.: phone, (217) 244-5360; fax, (217) 244-8068; e-mail, vddonk@uiuc.edu. T.R.H.: phone, (831) 459-5884; fax, (831) 459-2935; e-mail, tholman@chemistry.ucsc.edu.

[1]Abbreviations: LO, lipoxygenase; sLO-1, soybean lipoxygenase-1; 15-hLO-1, human reticulocyte 15-lipoxygenase-1; 12-hLO, human platelet 12-lipoxygenase; AA, arachidonic acid; 15-HPETE, 15(*S*)-hydroperoxyeicosatetraenoic acid; 15-HETE, 15(*S*)-hydroxyeicosatetraenoic acid; 12-HPETE, 12(*S*)-hydroperoxyeicosatetraenoic acid; 12-HETE, 12(*S*)-hydroxyeicosatetraenoic acid; d_4-AA, (10,10,13,13)-d_4-AA; LA, linoleic acid; d_{31}-LA, fully deuterated LA; 13-HPODE, 13(*S*)-hydroperoxyoctadecadienoic acid; 13-HODE, 13(*S*)-hydroxyoctadecadienoic acid; perdeuterated 13-HPODE, fully deuterated 13(*S*)-HPODE; perdeuterated 13-HODE, fully deuterated 13(*S*)-HODE; k_{cat}, rate constant for product release; k_{cat}/K_M, rate constant for fatty acid capture; $k_{cat}/K_M[O_2]$, rate constant for oxygen capture, $^Dk_{cat}/K_M$, kinetic isotope effect for k_{cat}/K_M; $^Dk_{cat}$, kinetic isotope effect for k_{cat}; RDS, rate-determining step.

 Published on Web 05/26/2009

Scheme 1

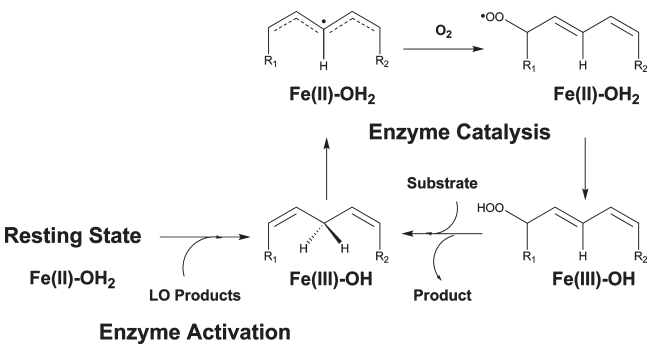

of sLO-1, and the kinetics of the reaction are best described as a "ping-pong-like" mechanism, where there is no formation of a ternary complex (*18*). At a low temperature (15 °C), the k_{cat}/K_M[LA] for sLO-1 has three partially rate-determining steps (RDS) consisting of diffusion, solvent sensitive hydrogen bonding rearrangements, and hydrogen atom abstraction (*19*), while k_{cat}[LA] is solely limited by hydrogen atom abstraction (*20*). At a high temperature (37 °C), both k_{cat}/K_M[LA] and k_{cat}[LA] are solely limited by hydrogen atom abstraction. 15-hLO-1 has been less extensively studied but appears to have similar kinetic behavior when LA is the substrate, with k_{cat}/K_M[LA] having multiple RDSs at low temperatures (hydrogen atom abstraction and hydrogen bonding rearrangement) but becoming solely limited by hydrogen atom abstraction at high temperatures (*21*). The k_{cat}[LA] for 15-hLO-1 is solely limited by hydrogen atom abstraction at all temperatures (*21*). It has been assumed that the hydrogen atom abstraction for 15-hLO-1 is irreversible and that a ternary complex is not formed, due to the general similarities between sLO-1 and 15-hLO-1, with LA as the substrate. Nevertheless, it is unclear if the similarities of the kinetic behavior between the two LOs, described above, extends to the native substrate for 15-hLO-1 and 12-hLO, AA.

To this end, our laboratories subsequently synthesized AA, dideuterated on C-13 (13,13-d_2-AA), and determined for sLO-1 that the $^{D}k_{cat}$ with AA was similar to that with LA (*22*). A large $^{D}k_{cat}$[AA] was observed with small activation energies, indicating a similar tunneling mechanism for the hydrogen atom abstraction of both substrates. Moreover, the extent of diffusion control on the k_{cat}/K_M[AA] was at a maximum at 20 °C, decreasing in prominence as the temperature increased or decreased, comparable to that of sLO-1 with LA as the substrate (*19*). In contrast, the $^{D}k_{cat}/K_M$[AA] for sLO-1 was shown to be small (~8) and temperature-independent, with no solvent isotope effect (SIE) at any temperature. These sLO-1 results with AA are distinct from the LA kinetics and can be partially explained by an increase in affinity for AA, which results in an increase in commitment, and a subsequent decrease in $^{D}k_{cat}/K_M$[AA] (*22*).

For 15-hLO-1, it was determined, using product branching experiments with d_4-AA, labeled at C10 and C13, that the $^{D}k_{cat}$[AA] was small in comparison to the $^{D}k_{cat}$[AA] for sLO-1, with a value of 11.6 ± 2.0 for C13 and 8.5 ± 4.0 for C10 hydrogen atom abstraction (*23*). These values were markedly lower than that seen with LA as the substrate (*21*) and raised the possibility of a different mechanism. It was recently observed that substrate specificity of 15-hLO-1 with AA and LA could be changed through product regulation of an allosteric site, and that 15-hLO-1 displays an increase in KIE for LA in the presence of the allosteric affector, 12-hydroxyeicosatetraenioc acid (12-HETE) (*14*). If the mechanisms of catalysis for AA and LA are fundamentally different and can be altered by the presence of allosteric effectors, then it is conceivable that this may help explain the change in substrate specificity of 15-hLO-1 and provide a method for investigating the effect of the allosteric site. To investigate whether the mechanistic behavior of the various LO isozymes, sLO-1, 15-hLO-1, and 12-hLO, is dependent on the type of substrate (LA vs AA) and whether allosteric effectors can alter catalytic profiles, we determined the kinetic isotope effect (KIE) and the solvent isotope effect (SIE) for both 15-hLO-1 and 12-hLO, with AA as the substrate, and determined the kinetic changes for 15-hLO-1 with allosteric effectors added.

MATERIALS AND METHODS

Materials. All commercial fatty acids (Sigma-Aldrich Chemical Co.) were repurified using a Higgins HAIsil Semi-Preparative (5 μm, 250 mm × 10 mm) C-18 column. Solution A was 99.9% MeOH and 0.1% acetic acid; solution B was 99.9% H_2O and 0.1% acetic acid. An isocratic elution of 85% A and 15% B was used to purify all fatty acids, which were stored at −80 °C for a maximum of 6 months. LO products were generated by reacting substrate with the appropriate LO isozyme (13-HPODE from sLO-1 and LA, 15-HPETE from sLO-1 and AA, and 12-HPETE from 12-hLO and AA). Product generation was performed as follows. An assay of 100 mL of 50−100 μM substrate was run to completion; reactions were quenched with 5 mL of acetic acid, and mixtures were extracted twice with 50 mL of dichloromethane, evaporated to dryness, and reconstituted in MeOH for HPLC purification. All products were tested with sLO-1 to show that no residual substrate was present and exhibited, by both analytical HPLC and liquid chromatography−tandem mass spectroscopy (LC−MS/MS), greater than 98% purity. The reduced products were generated by selectively reducing the 98% pure peroxide product to the alcohol, with trimethyl phosphite. The purity of the reduced hydroxy products was then confirmed via LC−MS/MS and by demonstrating no change in the lag phase of sLO-1 by hydroperoxide product activation. Perdeuterated LA (d_{31}-LA) (98% deuterated, Cambridge Isotope Laboratories) was purified as previously described (*24*). The (10,10,13,13)-d_4-AA (d_4-AA) was synthesized as previously described (*23*, *25*, *26*). All other chemicals were reagent grade or better and were used without further purification.

Overexpression and Purification of 15-Human Lipoxygenase-1 and 12-Human Lipoxygenase. Human reticulocyte 15-lipoxygenase-1 (15-hLO-1) and human platelet 12-lipoxygenase (12-hLO) were expressed as N-terminally, His_6-tagged proteins and purified to greater than 90% purity, as evaluated by sodium dodecyl sulfate−polyacrylamide gel electrophoresis (SDS−PAGE) analysis, as previously published (*27*, *28*). The iron content of 12-hLO and 15-hLO-1 was determined with a Finnigan inductively coupled plasma mass spectrometer (ICP-MS), using cobalt-EDTA as an internal standard. Iron concentrations were compared to standardized iron solutions and used to normalize enzyme concentrations.

Steady-State Kinetic Measurements. Lipoxygenase rates were determined by following the formation of the conjugated diene product at 234 nm (ε = 25000 M^{-1} cm^{-1}) with either a Perkin-Elmer Lambda 40 UV/vis or a Cary 100 Bio spectrophotometer. All reaction mixtures were 2 mL in volume and constantly stirred using a magnetic stir bar at room temperature (22 °C) unless otherwise described. Assays were conducted in

25 mM Hepes buffer (pH 7.5) with substrate concentrations ranging from 1 to 20 μM and were initiated by the addition of enzyme, as described below. The 12-hLO displays erratic behavior at low substrate concentrations (<1 μM), resulting in large errors in the K_M values. To circumvent this inherent problem, we determined that adding the 12-hLO first, and then quickly initiating the reaction with the addition of the appropriate amount of substrate, yielded significantly more reproducible results. Substrate concentrations were quantitatively determined by allowing the enzymatic reaction to go to completion. Kinetic data were obtained by recording initial enzymatic rates at each substrate concentration and were then fitted to the Michaelis–Menten equation using KaleidaGraph (Synergy) to determine k_{cat} and k_{cat}/K_M values.

Determination of the Kinetic Isotope Effect for 15-hLO-1 with AA as the Substrate. The noncompetitive kinetic isotope effect on the k_{cat} ($^{D}k_{cat}$[AA]) and k_{cat}/K_M ($^{D}k_{cat}/K_M$[AA]) values was determined by comparing the steady-state kinetic results of protiated arachidonic acid with that of d_4-arachidonic acid, as previously described (*19*, *21*). Kinetic measurements were performed using a Cary 100 Bio spectrophotometer by following product formation at 234 nm, at temperatures ranging from 15 to 40 °C in 25 mM Hepes buffer (pH 7.5). Reactions were initiated using ~16 and ~40 nM 15-hLO-1 (normalized to iron content) for protiated and tetradeuterated arachidonic acid, respectively, with substrate concentrations ranging from 1 to 15 μM. Reactions were performed in the presence of purified 13-HPODE (~6 μM) (or 15-HPETE, ~6 μM) to activate 15-hLO-1 and remove the kinetic lag phase. Kinetic parameters were determined as described in Steady-State Kinetic Measurements.

Determination of the Kinetic Isotope Effect for 12-hLO with AA as the Substrate. The noncompetitive kinetic isotope effect on the k_{cat} and k_{cat}/K_M values was determined as described above for 15-hLO-1. The steady-state KIE experiments were performed using a PE Lambda 40 spectrophotometer, using buffer conditions described above [25 mM Hepes (pH 7.5)] at temperatures ranging from 15 to 37 °C. Reactions were initiated using ~5 and ~60 nM 12-hLO (normalized to iron content) for protiated and tetradeuterated arachidonic acid, respectively, with substrate concentrations ranging from 0.1 to 10 μM. All kinetic parameters were determined as described in Steady-State Kinetic Measurements.

Determination of the Solvent Isotope Effect for 12-hLO and 15-hLO-1 with AA as the Substrate. The solvent isotope effect was determined by comparing the steady-state kinetic results of assays performed in H_2O and D_2O at temperatures ranging from 15 to 40 °C as previously described (*19*, *21*). Reactions were performed in 25 mM Hepes buffer (pH 7.5) (pH meter reading was 7.1 for buffered D_2O) and initiated using ~5 and ~7 nM enzyme (normalized to iron content) for 12-hLO and 15-hLO-1, respectively. All kinetic parameters were determined as described in Steady-State Kinetic Measurements. The variable-temperature SIE experiments for 15-hLO-1 included the addition of 13-HPODE (6 μM) to remove the kinetic lag phase. The SIE was also performed with and without 12-HETE (5 μM) at 15 °C, to determine if allosteric product binding affected the solvent dependency of the reaction.

Determining the Effects of 12-HETE on the Competitive Kinetic Isotope Effect and the Solvent Isotope Effect of 15-hLO-1 with AA as the Substrate. The $^{D}k_{cat}/K_M$[AA] ratio was determined in a manner similar to the previously published competitive substrate specificity method (*14*), which utilizes a Finnigan LTQ liquid chromatography-tandem mass spectrometer (LC–MS/MS) to quantify the product generation. The enzymatic reactions were initiated by the addition of 1 μM substrate, of a known molar ratio (1:1) of d_4-AA:AA, with and without preincubation of 12-HETE (5 μM) (or 13-HODE, 5 μM) with 15-hLO-1 (~4 nM). Enzymatic assays were performed using buffer conditions described above (25 mM Hepes, pH 7.5, 22 °C). A Phenomenex Synergi Hydro-RP (4 μm, 150 mm × 2.0 mm) column was used to detect the reduced LO products with an elution protocol consisting of 0.2 mL/min and an isocratic mobile phase of 59.9% ACN, 40% H_2O, and 0.1% THF. The corresponding reduced product ion peak ratio was determined using negative ion MS/MS (collision energy of 35 eV), with the following masses: 15-HETE, parent m/z = 319, fragments m/z = 175 and 219; 12-HETE, parent m/z = 319, fragments m/z = 179 and 257; 13-HODE, parent m/z = 295, fragments m/z = 183 and 251; and perdeuterated 13-HODE, parent m/z = 325, fragments m/z = 213 and 281 (*29*). All extracted reaction mixtures were reduced with trimethyl phosphite for LC–MS/MS analysis.

The effect of 12-HETE on the SIE of 15-hLO-1 was determined as described above; however, 12-HETE (5 μM) was added to each substrate concentration for steady-state kinetic analysis. Reactions were performed in 25 mM Hepes buffer (15 °C) at pH 7.5 (pH meter reading was 7.1 for D_2O) and initiated using ~40 nM enzyme (normalized to iron content) for 15-hLO-1.

Determining O_2 Kinetics for 15-hLO-1. Reaction rates of 15-hLO-1 with AA and LA were determined by measuring the extent of oxygen consumption on a Clark oxygen monitor as previously described (*30*). Reactions were conducted as a function of oxygen concentrations in 1 mL solutions, which were stirred constantly and equilibrated under air at 25 °C (258 μM O_2). The reaction was initiated by addition of ~30 nM 15-hLO-1 (normalized to iron content), via a gastight Hamilton syringe to the reaction chamber. The experiments were repeated at variable concentrations of oxygen, established by passing mixtures of N_2 and O_2 over stirred solutions in the reaction chamber for 10 min. The established oxygen concentration was calibrated against the value of O_2 dissolved in an air-saturated solution at 25 °C (258 μM O_2). The rate of oxygen consumption was recorded at oxygen concentrations ranging from 5 to 500 μM, in 25 mM Hepes (pH 7.5, 25 °C) and saturating substrate conditions (25 μM). Further investigations were performed in the presence of 12-HETE (5 μM), to determine if allosteric binding affected the $K_M[O_2]$, with either substrate.

Lag Phase Investigations of 15-hLO-1. Observations that 15-hLO-1 has an extended lag phase (activation period) with AA as compared to LA prompted us to investigate if this effect is due to differences in their affinity toward the ferrous enzyme (resting-state enzyme), as previously seen with sLO-1 (*22*). Reactions were conducted as described for the steady-state experiments (25 mM Hepes, pH 7.5, 22 °C), initiating the assays by adding 15-hLO-1 to final concentrations of 12 and 18 nM (normalized to iron content, to achieve similar initial rates) for LA and AA, respectively, under substrate limiting conditions (5 μM). The 15-hLO-1 enzyme was then preincubated (<5 s, to avoid observable turnover) with AA (25 μM), followed by addition of LA, and vice versa, to determine the effect on the lag phase, as previously described (*22*).

RESULTS AND DISCUSSION

Mechanistic Investigations of Human 15-Lipoxygenase-1 with AA as the Substrate. (i) Noncompetitive Kinetic Isotope Effect. Previous variable-temperature KIE studies with LO isozymes were limited to deuterated linoleic acid (*19*, *21*, *24*), since appropriately deuterated AA is not commercially available and is difficult to synthesize. In this study, (10,10,13,13)-d_4-arachidonic acid (d_4-AA) was synthesized as previously described (*23*, *25*, *26*) and utilized to investigate the KIE of 15-hLO-1 and 12-hLO. Deuterium labeling at both C10 and C13 was required to prevent changes in regioselectivity (*23*). Since both carbons are dideuterated, the observed KIE results include both primary and secondary effects. It should be noted that the secondary KIE will likely not make a large contribution to the observed KIE, since oxidation of LA by sLO-1 was previously shown to exhibit a small secondary effect (*20*). Investigations of 15-hLO-1 with LA have previously demonstrated a temperature-dependent $^{D}k_{cat}/K_M$[LA] and k_{cat}/K_M[LA] SIE and a temperature-independent $^{D}k_{cat}$[LA] (~40) and k_{cat}[LA] SIE (*21*). These studies suggest 15-hLO-1 displays hydrogen atom tunneling and has multiple RDSs at low temperatures for k_{cat}/K_M[LA], whereas the k_{cat}[LA] is solely rate-limited by hydrogen atom abstraction. In this work, the noncompetitive, variable-temperature KIE of 15-hLO-1 with AA was significantly different than the 15-hLO-1/LA data, demonstrating temperature dependency for both $^{D}k_{cat}/K_M$[AA] and $^{D}k_{cat}$[AA] and with markedly lower magnitudes (Figure 1). The $^{D}k_{cat}/K_M$[AA] was determined to be 6.3 ± 2.5, 6.0 ± 1.5, 9.0 ± 1.6, 10.0 ± 2.3, 3.6 ± 1.5, and 4.5 ± 2.0 for 15, 20, 25, 30, 35, and 40 °C, respectively. The $^{D}k_{cat}$[AA] data were determined to be 6.7 ± 0.6, 8.6 ± 0.6, 8.9 ± 1.1, 10.3 ± 0.7, 8.9 ± 1.4, and 6.6 ± 0.9 for 15, 20, 25, 30, 35, and 40 °C, respectively.

The temperature dependence of $^{D}k_{cat}/K_M$[AA] and $^{D}k_{cat}$[AA] is suggestive of multiple rate-limiting steps, as seen by the increase and then decrease of $^{D}k_{cat}/K_M$[AA] and $^{D}k_{cat}$[AA] as the temperature increases above 30 °C. The magnitudes of both $^{D}k_{cat}/K_M$[AA] and $^{D}k_{cat}$[AA] for 15-hLO-1 are considerably smaller than the previously reported $^{D}k_{cat}/K_M$[LA] and $^{D}k_{cat}$[LA] values for 15-hLO-1 (*21*), suggesting a different mechanistic behavior between AA and LA. Unfortunately, it is difficult to probe this mechanistic difference thoroughly with ΔE_{act} and A_H/A_D investigations, as was reported for sLO-1 and 15-hLO-1 with LA (*21*, *31*), due to multiple RDSs for the k_{cat}[AA] of 15-hLO-1 at low temperatures (vide infra). Moreover, the observed inactivation of 15-hLO-1 with AA at high temperatures makes the energy of activation (E_{act}) and the Arrhenius prefactor (A) for d_4-AA unattainable. Therefore, caution should be used when interpreting the temperature dependence data in Figure 1, since it does not reflect the intrinsic KIE.

The variable-temperature, noncompetitive KIE data for 15-hLO-1 with AA were obtained in the presence of 13-HPODE (6 μM) to remove the kinetic lag phase, which is more pronounced with AA than with LA. However, this raises the concern that binding of 13-HPODE to the allosteric site may be affecting the observed KIE, which was seen previously with the addition of 12-HPETE or 12-HETE to 15-hLO-1 and LA (*14*). The noncompetitive KIE study was therefore performed in the presence of 15-HPETE (6 μM) in 25 mM Hepes (pH 7.5, 25 °C), which demonstrated that addition of 15-HPETE afforded very similar KIE results as with 13-HPODE added ($^{D}k_{cat}/K_M$[AA] = 11 ± 2, and $^{D}k_{cat}$[AA] = 7.3 ± 0.6).

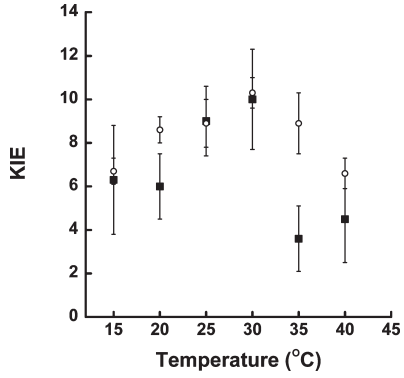

FIGURE 1: Temperature dependence of the observed KIE for 15-hLO-1: $^{D}k_{cat}$ (○) and $^{D}k_{cat}/K_M$ (■). Enzymatic assays were performed in 25 mM Hepes buffer (pH 7.5) with addition of 13-HPODE (6 μM).

(ii) Competitive Kinetic Isotope Effect. To confirm the $^{D}k_{cat}/K_M$[AA] value of 15-hLO-1, the competitive $^{D}k_{cat}/K_M$[AA] was determined with a mixture of d_4-AA and AA at 22 °C, using the LC−MS/MS method previously described for substrate specificity studies (*14*). Using d_4-AA, the $^{D}k_{cat}/K_M$[AA] values were determined to be 8 ± 1 and 10 ± 2 for abstraction from C13 and C10, respectively (Figure S1 of the Supporting Information). These values are in good agreement with the observed noncompetitive KIE data (the average KIE for both C13 and C10) and with the previously published $^{D}k_{cat}$[AA] values from product branching experiments (*23*). Considering that no product was added to the competitive experiments and yet the $^{D}k_{cat}/K_M$[AA] value was the same as the noncompetitive results, which had both 13-HPODE and 15-HPETE added, the data indicate that there was no allosteric effect on the $^{D}k_{cat}/K_M$[AA] of 15-hLO-1 with the addition of these LO products.

The low KIE values, relative to $^{D}k_{cat}/K_M$[LA], could be due to a variety of reasons, including a large kinetic commitment with AA as previously seen for sLO-1 (*22*), a decreased contribution of the abstraction step to the rate-limiting step (*19*), or a change in the activation barrier shape (*32*). To probe this further, 12-HETE (5 μM) was added to the competitive reaction mixture of d_4-AA/AA with 15-hLO-1, and the observed $^{D}k_{cat}/K_M$[AA] increased from 8 ± 1 to 18 ± 3, clearly indicating that tunneling is involved in the hydrogen atom abstraction process. A similar result was previously observed with the addition of 12-HPETE or 12-HETE to 15-hLO-1, with $^{D}k_{cat}/K_M$[LA] increasing from 24 to 44 (*14*). It should be noted that 13-HODE was also added to the competitive peroxidation of d_4-AA/AA by 15-hLO-1 and was shown to have little effect on $^{D}k_{cat}/K_M$[AA] (10 ± 2), confirming the noncompetitive KIE result (vide supra).

(iii) Solvent Isotope Effect. It was previously shown that the reaction of 15-hLO-1 with LA (no 13-HPODE added) displayed a temperature-dependent k_{cat}/K_M[LA] SIE yet no SIE for k_{cat}[LA], indicating that k_{cat}/K_M[LA] is partially rate-limited by a solvent-dependent step while k_{cat}[LA] is not (*21*). In contrast, the results for 15-hLO-1 with AA (13-HPODE added) demonstrate a temperature-dependent SIE for both k_{cat}/K_M[AA] and k_{cat}[AA], indicating multiple rate-limiting steps at low temperatures for both kinetic parameters. The SIE values range from 2.2 ± 0.4 to 1.1 ± 0.3 for k_{cat}/K_M and from 2.0 ± 0.2 to 1.1 ± 0.1 for k_{cat} (Figure 2). This observation is consistent with the $^{D}k_{cat}/K_M$[AA] and $^{D}k_{cat}$[AA] temperature dependence data. The observed SIE at lower temperatures also explains the decreased substrate KIE values at low temperatures, as a solvent-dependent

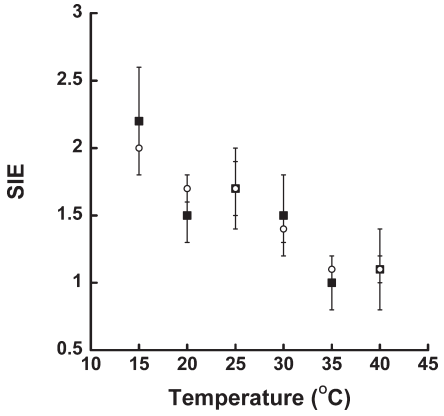

FIGURE 2: Temperature dependence of the solvent isotope effect for 15-hLO-1: k_{cat} (○) and k_{cat}/K_M (■). Enzymatic assays were performed in 25 mM Hepes buffer (pH 7.5) with addition of 13-HPODE (6 μM).

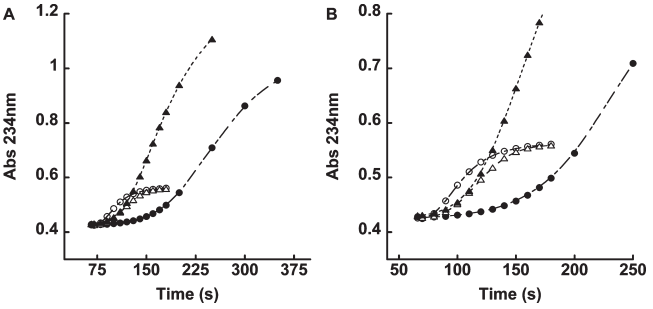

FIGURE 3: (A) Lag phase comparison of 15-hLO-1 with AA (5 μM) (△) and LA (5 μM) (○). Preincubation with AA (25 μM) followed by addition of LA (5 μM) (●) and preincubation of LA (25 μM) followed by addition of AA (5 μM) (▲). (B) Magnified view of 15-hLO-1 lag phase data. Enzymatic assays were performed in 25 mM Hepes buffer (pH 7.5, 22 °C).

step would partially mask the observed KIE of the hydrogen atom abstraction step, since abstraction is not fully rate-limiting. The SIE data, however, do not explain the decreasing substrate KIE values at high temperatures, since there is no SIE effect in this temperature range (vide infra).

As discussed above, the addition of 12-HETE increased the competitive $^{D}k_{cat}/K_M$[AA] considerably, whereas 13-HPODE and 15-HPETE had little effect on the $^{D}k_{cat}/K_M$[AA]. The effect of 12-HETE on the reaction mechanism of 15-hLO-1 was investigated further by probing the SIE at low temperatures (15 °C), where the SIE was greatest. It was determined that the addition of 12-HETE [5 μM, 5 times the allosteric K_D (*14*)] significantly lowered the SIE (15 °C) to 1.4 ± 0.2 and 1.4 ± 0.2 for k_{cat}/K_M[AA] and k_{cat}[AA], respectively. This indicates that the solvent-dependent step for 15-hLO-1 has become less rate-limiting with the addition of 12-HETE and corroborates the competitive $^{D}k_{cat}/K_M$[AA] results that show an increased substrate KIE with the addition of 12-HETE.

(iv) Determining O_2 Kinetics for 15-hLO-1. Previously, our laboratories performed O_2 dependency experiments for the oxidation of LA by 15-hLO-1 and AA by 12-hLO and determined the $K_M[O_2]$ values to be 4.2 ± 1.1 and 7.0 ± 1.4 μM, respectively ([fatty acid] = 25 μM, at 25 °C) (*21*). In the investigation presented here, 15-hLO-1 was studied with AA and LA (25 °C) concurrently, for direct comparison, and the $K_M[O_2]$ was determined to be more than 2-fold greater for AA than for LA (Table 1). The k_{cat} values were determined and are in agreement with k_{cat} values determined spectrophotometrically (*14*). The $k_{cat}/K_M[O_2]$ values therefore indicated a greater than 3-fold preference for LA, under oxygen limiting conditions. The addition of 12-HETE (5 μM) demonstrated a decrease in the $k_{cat}/K_M[O_2]$ for LA (an increase in $K_M[O_2]$) and an increase in the $k_{cat}/K_M[O_2]$ for AA (a decrease in $K_M[O_2]$), yielding similar $k_{cat}/K_M[O_2]$ values for both LA and AA (Table 1). This is a remarkable result since the binding of 12-HETE to the allosteric site not only increases the fatty acid $(k_{cat}/K_M)^{AA}/(k_{cat}/K_M)^{LA}$ ratio 4-fold (*14*) but also increases the oxygen $(k_{cat}/K_M)^{AA}/(k_{cat}/K_M)^{LA}$ ratio 3-fold, which indicates a dramatic change in the substrate specificity of 15-hLO-1 toward AA. The k_{cat} values showed little effect with the addition of 12-HETE and are in agreement with the previously published spectroscopic data (*14*). It should be noted that with sLO-1, saturating amounts of 13-HPODE were required for maximal $k_{cat}/K_M[O_2]$ (*30*), which was explained to be due to loss of the substrate radical, generating the inactive ferrous enzyme. This hypothesis was consistent with the data; however, it is possible that in addition, the product is binding to the allosteric site of sLO-1. Further investigations are needed to determine if the allosteric site is also playing a role with sLO-1.

Table 1: Comparison of the Steady-State Kinetic Parameters of 15-hLO-1 for Oxygen with AA and LA as Substrates[a]

	no product addition	12-HETE addition
	AA	
k_{cat} (s^{-1})	5.6 ± 0.2	5.1 ± 0.1
$K_M[O_2]$ (μM)	24 ± 3	15 ± 1
$k_{cat}/K_M[O_2]$ (s^{-1} μM^{-1})	0.23 ± 0.04	0.34 ± 0.03
	LA	
k_{cat} (s^{-1})	7.6 ± 0.1	7.0 ± 0.3
$K_M[O_2]$ (μM)	9.6 ± 0.6	22 ± 4
$k_{cat}/K_M[O_2]$ (s^{-1} μM^{-1})	0.79 ± 0.08	0.32 ± 0.07

[a] Enzymatic assays were performed in 25 mM Hepes buffer (pH 7.5, 25 °C), with and without product addition, in the presence of 25 μM substrate. Oxygen consumption was detected using a Clark oxygen monitor.

(v) Lag Phase Investigations. As mentioned, AA demonstrates a higher affinity for the ferrous sLO-1 enzyme than LA, manifested by a difference in their lag phase (*22*). This observation suggested that AA had a smaller K_D than LA for the ferrous enzyme, which could increase the commitment with AA, consequently lowering the observed $^{D}k_{cat}/K_M$[AA]. As seen in Figure 3, 15-hLO-1 also displays a longer lag phase with AA than with LA, at low substrate concentrations. Preincubation of 15-hLO-1 with LA (25 μM) followed by AA addition (5 μM) had the same lag phase as pure AA (5 μM), whereas a large increase in the lag phase is seen with preincubation with AA (25 μM), followed by addition of LA (5 μM). These data suggest that the affinity of AA for the ferrous 15-hLO-1 is at least 5-fold greater than that of LA, since 5 μM AA outcompetes 25 μM preincubated LA (Figure 3A, B). Interestingly, the LO products, 13-HPODE and 12-HPETE, were shown to eliminate the lag phase for 15-hLO-1 with AA, but the reduced products, 13-HODE and 12-HETE, did not, suggesting that allosteric binding does not affect the lag phase. Finally, no autoinactivation of 15-hLO-1 was observed with either AA or LA at low substrate concentrations; however, AA autoinactivates 15-hLO-1 to a much greater extent than LA at high substrate concentrations, as seen by the lower level of overall product generation (Figure 3A). This difference may indicate that

the autoinactivation with AA is not relevant for cellular processes since the low substrate concentration is more similar to that seen in the cell.

(vi) Summary of 15-hLO-1. The observed KIE for 15-hLO-1, with AA as its substrate, demonstrates that the kinetic behavior of 15-hLO-1 with AA is remarkably different from its kinetic behavior with LA as its substrate (*21*). The $^{D}k_{cat}$[AA] and $^{D}k_{cat}/K_M$[AA] values are small and temperature-dependent, with decreasing $^{D}k_{cat}/K_M$[AA] and $^{D}k_{cat}$[AA] values at both low and high temperatures, suggesting that hydrogen atom abstraction is not the sole RDS. At low temperatures, the decrease in $^{D}k_{cat}/K_M$[AA] and $^{D}k_{cat}$[AA] is partially due to a hydrogen bonding rearrangement step, as seen by the large SIE at low temperatures. However, at high temperatures, no SIE was observed for either k_{cat}/K_M or k_{cat}, indicating hydrogen bonding rearrangement is not responsible for the decrease in $^{D}k_{cat}/K_M$[AA] or $^{D}k_{cat}$[AA]. This decrease in the observed KIE values could be due to inactivation of 15-hLO-1 at high temperatures or diffusion being a rate-determining step, but unfortunately, the diffusion step cannot be investigated because the available viscogens affect catalysis (*21*).

These results are distinct from the 15-hLO-1/LA kinetic results, in that both k_{cat}/K_M and k_{cat} for 15-hLO-1/AA are sensitive to solvent (i.e., SIE) and that the values of $^{D}k_{cat}/K_M$[AA] and $^{D}k_{cat}$[AA] are significantly lower than the values with LA as the substrate (*21*). This latter issue was probed further by investigating the lag phase of 15-hLO-1. Previously, our laboratories postulated that the $^{D}k_{cat}/K_M$[AA] for sLO-1 was masked by a large commitment (k_3/k_2; vide infra), since AA appeared to bind more tightly to the ferrous sLO-1 species than LA, extending the lag phase (*22*). This experiment was repeated with 15-hLO-1, and it was observed that AA also extended the lag phase of LA catalysis. This result corroborates the hypothesis that AA binds more tightly to 15-hLO-1 than LA and therefore 15-hLO-1 could have a larger commitment (k_3/k_2) with AA. Commitment (k_3/k_2) can be defined by examining the proposed mechanism of 15-hLO-1 (Scheme 2). This scheme assumes that hydrogen atom abstraction is irreversible, with no ternary complex formation, and that the substrate radical ($L^{\bullet}$) has a high affinity, as demonstrated for sLO-1 (*18*, *30*).

Scheme 2

$$E + LA \underset{k_2}{\overset{k_1[LA]}{\rightleftharpoons}} ELA \xrightarrow{k_3} EL^{\bullet} \underset{k_6}{\overset{k_5[O_2]}{\rightleftharpoons}} ELOO^{\bullet} \underset{k_8}{\overset{k_7}{\rightleftharpoons}} ELOOH \xrightarrow{k_9} E+P$$

$$KIE = {}^{D}k_{cat}/K_M = (k_{cat}/K_M)^{H}/(k_{cat}/K_M)^{D} = (k_3^{H}/k_3^{D} + k_3^{H}/k_2^{H})/(1 + k_3^{H}/k_2^{H}) \quad (1)$$

According to Scheme 2, $^{D}k_{cat}/K_M$ would be defined by eq 1, where substrate release (k_2) and hydrogen atom abstraction (k_3) are the primary determinants for $^{D}k_{cat}/K_M$ (assuming k_3 is irreversible, a ternary complex is not formed, and the multiple steps observed at low temperatures are included in k_3). The $^{D}k_{cat}/K_M$ increases to a maximum of k_3^{H}/k_3^{D} when commitment (k_3/k_2) is small and decreases to a value approaching 1 when commitment for 15-hLO-1 with AA is large, assuming that the intrinsic k_3^{H}/k_3^{D} remains unchanged (eq 1). Therefore, a large commitment for 15-hLO-1 with AA would lower the observed KIE and potentially mask a large intrinsic KIE. It should be noted that the small observed KIE for 15-hLO-1 and AA does not necessarily exclude the possibility of tunneling (*33*−*36*). Another possible explanation could be a change in the shape of the potential energy barrier. Sutcliffe and Scrutton postulate that the small KIE value of aromatic amine dehydrogenase (AADH) with certain substrates could be due to a change in the shape of the potential energy barrier (*32*), which could also be occurring with 15-hLO-1 and AA.

The small $^{D}k_{cat}/K_M$[AA] was investigated further by adding the allosteric effector molecule, 12-HETE, which increased the observed $^{D}k_{cat}/K_M$[AA] from 8 to 18. This latter value is well above the semiclassical prediction (*37*, *38*) and suggests that the hydrogen atom abstraction of AA by 15-hLO-1 is occurring through a tunneling mechanism, once 12-HETE is added. The reason for the increase in the KIE is most likely not due to a decrease in commitment, as seen for sLO-1 with AA (*22*), since addition of 12-HETE decreases the K_M[AA] (*14*), which in the framework of Scheme 2 would have the opposite effect on commitment. Moreover, it was observed that while 13-HPODE and 12-HPETE reduced the kinetic lag phase for 15-hLO-1 with AA, 13-HODE and 12-HETE did not. This observation indicated that the release rate of AA (k_2), and hence commitment, was not changing upon allosteric binding.

The SIE of 15-hLO-1 was subsequently probed via the addition of 12-HETE to determine if the allosteric site affected the relative contributions of the partially rate-limiting steps. Interestingly, the k_{cat}/K_M[AA] SIE was observed to decrease from 2.2 to 1.4, indicating that 12-HETE binding decreases the contribution of the solvent dependency to the overall rate and increases the contribution of hydrogen atom abstraction. This increase in contribution of hydrogen atom abstraction to the overall rate is also exhibited by an increased observed KIE upon addition of 12-HETE. It should be noted that previously our laboratories demonstrated that 12-HETE increased the observed KIE for 15-hLO-1 with LA (*14*), and we postulated that the increase was due to a decrease in commitment, as seen by the decrease in k_{cat}[LA] (i.e., k_3). Given the current data, it is possible that the loss of the solvent-dependent step could also be contributing to the increase in the observed KIE with 15-hLO-1 and LA, and further studies are required. The change in the $^{D}k_{cat}/K_M$ for 15-hLO-1 with AA upon addition of 12-HETE could also be due to a change in the shape of the potential energy barrier as seen for AADH (*32*), but this cannot be probed using the temperature dependency of k_{cat}, as previously done for sLO-1 and 15-hLO-1 with LA (*21*, *31*), since k_{cat} for 15-hLO-1 with AA is not fully rate-limited by hydrogen atom abstraction and 15-hLO-1 autoinactivates at high temperatures with AA.

Interestingly, 13-HPODE does not increase the $^{D}k_{cat}/K_M$[AA], nor does it decrease the SIE, even though it has an allosteric effect on substrate specificity, like 12-HETE (*14*). This result is unusual since one would suspect the KIE for the abstraction step to be more sensitive to allosteric binding than the change in substrate specificity. These results may suggest that 12-HETE and 13-HPODE affect the microscopic rate constants differently upon binding to the allosteric site and that their effect on substrate specificity is not necessarily linked to the change in the solvent-dependent, hydrogen bonding rearrangement step. Additional investigations are in progress to probe these results further.

Previously, our laboratories determined that the $^{D}k_{cat}$[AA] values for abstraction of a hydrogen atom from C10 and C13 were comparable (*23*). In the investigation presented here, we observe that the competitive $^{D}k_{cat}/K_M$[AA] for abstraction of a hydrogen atom from C10 is also comparable to that for

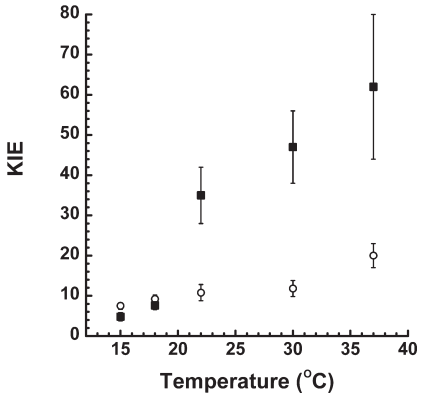

FIGURE 4: Temperature dependence of the observed KIE for 12-hLO: $^{D}k_{cat}$ (○) and $^{D}k_{cat}/K_M$ (■). Enzymatic assays were performed in 25 mM Hepes buffer (pH 7.5).

abstraction from C13 (*23*). These results suggest that the hydrogen atom abstraction at these two structurally distinct positions is of a comparable mechanism. This finding is unexpected since the active site would have to spatially accommodate these two disparate positions for the same hydrogen atom abstraction process. A previously postulated explanation for abstraction from different positions is that the substrate can bind in two conformations, head-first or tail-first (*39*). Another possible explanation could be that the intrinsic KIEs for these two carbon centers are in fact different, and the similarities in the observed KIE values reported in this work are due to masking of their intrinsic KIE values. We are currently investigating these possibilities further.

Another difference between 15-hLO-1 kinetics with AA and LA is the difference in their $k_{cat}/K_M[O_2]$ values. The $k_{cat}/K_M[O_2]$ for AA is more than 3-fold smaller than that of LA. This ratio is similar to that seen for sLO-1, whose $k_{cat}/K_M[O_2]$ is more than 9-fold less for AA than for LA (under saturating conditions of 13-HPODE) (*40*). However, the addition of 12-HETE increases the $k_{cat}/K_M[O_2]$ value of 15-hLO-1 with AA and decreases the $k_{cat}/K_M[O_2]$ value for LA, such that their $k_{cat}/K_M[O_2]$ values become near-equivalent for both substrates. This result is due to a change in $K_M[O_2]$ and may be relevant for human disease models since the oxygen concentration varies from 20 μM in normal tissue (*41*) to as low as 6 μM in prostate cancer (*42*), and hence, oxygen concentration could contribute to the regulation of LO substrate specificity in the cell.

The change in the $K_M[O_2]$ upon 12-HETE binding also has relevance for the microscopic steps of the oxidative half-reaction. Previously, Klinman and co-workers demonstrated with sLO-1 that the oxidative half-reaction consisted of the following microscopic steps (Scheme 2): O_2 reversibly diffuses to the surface of sLO-1 and then moves through the O_2 channel (included in k_5); O_2 reacts with the intermediate radical ($L^\bullet$) to form $LOO^\bullet$ (proposed as the RDS) (included in k_5); transfer of a hydrogen atom to $LOO^\bullet$ to form LOOH (k_7); and release of product (k_9) (*30*). Assuming that 15-hLO-1 has a ping-pong-like mechanism similar to that of sLO-1 (Scheme 2), as is suggested for rabbit 15-LO (*43*), then oxygen reacts with the fatty acid radical after the irreversible hydrogen atom abstraction, with no formation of a ternary complex and with no observable loss of the fatty acid radical. Therefore, if the fatty acid is saturating, as is used in our experiments, then all of the enzyme will be in the $EL^\bullet$ complex, the $k_{cat}/K_M[O_2]$ will be independent of fatty acid concentration, and the microscopic rate constants

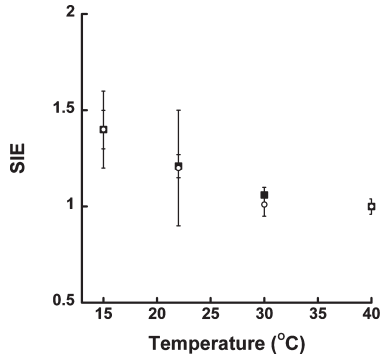

FIGURE 5: Temperature dependence of the solvent isotope effect of 12-hLO: $^{D}k_{cat}$ (■) and $^{D}k_{cat}/K_M$ (○). Enzymatic assays were performed in 25 mM Hepes buffer (pH 7.5).

can be expressed as follows:

$$k_{cat}[O_2] = \frac{k_3k_7k_9}{k_7k_9 + k_3k_8 + k_3k_9 + k_3k_7} \quad (2)$$

$$K_M[O_2] = \frac{k_3(k_6k_8 + k_7k_9 + k_6k_9)}{k_5(k_7k_9 + k_3k_8 + k_3k_9 + k_3k_7)} \quad (3)$$

$$k_{cat}/K_M[O_2] = \frac{k_5k_7k_9}{k_6k_8 + k_7k_9 + k_6k_9} \quad (4)$$

Considering that $k_{cat}[O_2]$ decreases only slightly for both substrates upon addition of 12-HETE, the effect of allosteric binding on $k_{cat}/K_M[O_2]$ arises primarily from changes in $K_M[O_2]$. However, since $K_M[O_2]$ is a kinetically complex parameter, 12-HETE binding could affect a variety of steps in the oxidative half-reaction. For example, the allosteric site could change either the position of the substrate relative to the O_2 channel or the nature of the O_2 channel itself, such that the attack of O_2 on $L^\bullet$ is affected. An added complication is that if hydrogen atom abstraction is not irreversible, as is assumed above, then the rate constant for $k_{cat}/K_M[O_2]$ could also include microscopic steps in the reductive half-reaction. Currently, we are investigating the O_2 kinetics further for both 15-hLO-1 and 12-hLO to determine their RDS and how the allosteric site may affect them.

Mechanistic Investigations of Human 12-Lipoxygenase with AA as the Substrate. (i) Noncompetitive Kinetic Isotope Effect. Variable-temperature KIE experiments demonstrated that the $^{D}k_{cat}/K_M$[AA] and $^{D}k_{cat}$[AA] of 12-hLO were temperature-dependent, with values ranging from 4.8 ± 0.9 to 62 ± 18 and from 7.5 ± 0.8 to 20 ± 3 between 15 and 37 °C, respectively (Figure 4).

The magnitudes of both $^{D}k_{cat}/K_M$[AA] and $^{D}k_{cat}$[AA], at high temperatures, indicate hydrogen atom tunneling, as previously seen for both sLO-1 and 15-hLO-1 with LA (*19*, *21*). The temperature dependence of both $^{D}k_{cat}/K_M$[AA] and $^{D}k_{cat}$[AA] for 12-hLO is suggestive of multiple RDSs in the reaction mechanism which have different contributions to the overall rate at the different temperatures.

(ii) Solvent Isotope Effect. Previously, our laboratories determined that 12-hLO displayed a temperature-dependent SIE for k_{cat}[AA], but a temperature-independent k_{cat}/K_M[AA] SIE, albeit with a large degree of error (*21*). However, in this study, 12-hLO exhibited a temperature-dependent KIE for both $^{D}k_{cat}/K_M$[AA] and $^{D}k_{cat}$[AA], suggesting a possible discrepancy between these two results. Considering that the original SIE

Table 2: Summary of the Observed Kinetic Behaviors for the Lipoxygenase Enzymes

	k_{cat}/K_M			k_{cat}	
	diffusion (viscosity)[a]	H bond rearrangement (observed SIE)[b]	H atom abstraction (observed KIE)[b]	H bond rearrangement (observed SIE)[b]	H atom abstraction (observed KIE)[b]
sLO-1/LA[c]	48% (20 °C)	3.7 (5 °C)	30 (25 °C)	2.2 (5 °C)	48 (25 °C)
sLO-1/AA[d]	56% (20 °C)	1.0 (Ind.)	8 (Ind.)	1.0 (Ind.)	150 (5 °C)
15-hLO-1/AA	ND[e]	2.2 (15 °C)	10 (30 °C)	2.0 (15 °C)	10 (30 °C)
12-hLO/AA	ND[e]	1.4 (15 °C)	50 (40 °C)	1.4 (15 °C)	20 (37 °C)

[a] Data are presented as percent diffusion limited at the temperature that the maximum effect was observed. [b] The SIE and KIE data are the observed values at the temperature of the maximal effect. Ind., temperature-independent kinetic parameter. [c] Data were obtained from ref (*19*), but it should be noted that subsequent work (*20*) with recombinant sLO-1 showed different k_{cat} values. [d] Data were obtained from ref (*22*). [e] Not determined.

data (*21*) and the current KIE data were determined under different conditions [25 mM Tris (pH 7.5) and 25 mM Hepes (pH 7.5), respectively], the SIE experiments were re-examined using the KIE reaction conditions used in this investigation. Under these new conditions, the error was reduced considerably and the solvent isotope effect for 12-hLO at pH 7.5 was determined to be 1.4 ± 0.1 and 1.4 ± 0.2 at 15 °C for k_{cat}/K_M[AA] and k_{cat}[AA], respectively. The SIE decreased with increasing temperature to 1.01 ± 0.04, for both k_{cat}/K_M[AA] and k_{cat}[AA] (Figure 5). The new SIE data correlate well with the substrate KIE data, providing further support for multiple, partially rate-limiting steps at low temperatures for both k_{cat}/K_M[AA] and k_{cat}[AA].

(iii) Summary of 12-hLO. These results demonstrate that 12-hLO is distinct from 15-hLO-1 not only in both its fatty acid selectivity (only reacting with AA) and its primary sequence (80% similar) but also in its kinetic behavior with AA. Our data demonstrate that both $^{D}k_{cat}/K_M$ and $^{D}k_{cat}$ for 12-hLO increase to large values at high temperatures, whereas the KIE for 15-hLO-1 with AA is at a maximum at 30 °C. However, the catalytic mechanism of 12-hLO is similar to that of 15-hLO-1 with AA in that its hydrogen atom abstraction proceeds through a tunneling mechanism, and both isozymes demonstrate a solvent-dependent step for both k_{cat}/K_M and k_{cat}, at low temperatures. Interestingly, the magnitude of the SIE value for 12-hLO, at 15 °C, is lower than that for 15-hLO-1, suggesting a weaker participation in the rate-limiting step. Unfortunately, it could not be determined if diffusion is also a rate-limiting step, as seen for sLO-1 with both LA and AA (*19*, *22*), since viscogens inhibit catalysis by 12-hLO (*21*).

CONCLUSION

In conclusion, this study reports three important findings with human lipoxygenase. First, both 15-hLO-1/AA and 12-hLO/AA have multiple RDSs at low temperatures (hydrogen atom abstraction and hydrogen bond rearrangement), and for both systems, the abstraction appears to proceed through a tunneling mechanism. However, the magnitude of the $^{D}k_{cat}/K_M$[AA] for 15-hLO-1 is significantly lower than that of 12-hLO. These data, coupled with the previously published sLO-1/AA data (*22*), indicate that there are mechanistic differences in sLO-1, 15-hLO-1, and 12-hLO, with the two substrates (AA and LA), even though hydrogen atom tunneling is a common mechanistic feature. Second, the binding of 12-HETE to the allosteric site of 15-hLO-1 decreases the contribution of the solvent-dependent step to the overall reaction rate, such that hydrogen atom abstraction (KIE) becomes the predominant RDS. Finally, 12-HETE increases the AA/LA ratio for $k_{cat}/K_M[O_2]$ with 15-hLO-1, such that there is no substrate preference between LA and AA, under limiting oxygen concentrations. These results, as well as our previous discovery that 12-HETE increases the AA/LA ratio for k_{cat}/K_M[fatty acid] (*14*), suggest that under cellular conditions (low fatty acid and low oxygen concentrations), the allosteric binding of 12-HETE to 15-hLO-1 could increase the substrate specificity of 15-hLO-1 toward AA over LA significantly, which may have important implications in cancer progression.

ACKNOWLEDGMENT

We gratefully acknowledge J. Klinman for the use of the Clark O_2 electrode and J. Klinman and M. Meyer helpful comments in the preparation of the manuscript.

SUPPORTING INFORMATION AVAILABLE

LC−MS/MS chromatogram for the 15-hLO-1 competitive kinetic isotope effect experiments ($^{D}k_{cat}/K_M$[AA]), used to determine the KIE for both C10 and C13 on arachidonic acid. This material is available free of charge via the Internet at http://pubs.acs.org.

REFERENCES

(1) Solomon, E. I., Zhou, J., Neese, F., and Pavel, E. G. (1997) New insights from spectroscopy into the structure/function relationships of lipoxygenases. *Chem. Biol. 4*, 795–808.
(2) Serhan, C. N. (1994) Lipoxin biosynthesis and its impact in inflammatory and vascular events. *Biochim. Biophys. Acta 1212*, 1–25.
(3) Nakano, H., Inoue, T., Kawasaki, N., Miyataka, H., Matsumoto, H., Taguchi, T., Inagaki, N., Nagai, H., and Satoh, T. (2000) Synthesis and biological activities of novel antiallergic agents with 5-lipoxygenase inhibiting action. *Bioorg. Med. Chem. 8*, 373–380.
(4) Ghosh, J., and Myers, C. E. (1998) Inhibition of arachidonate 5-lipoxygenase triggers massive apoptosis in human prostate cancer cells. *Proc. Natl. Acad. Sci. U.S.A. 95*, 13182–13187.
(5) Steele, V. E., Holmes, C. A., Hawk, E. T., Kopelovich, L., Lubet, R. A., Crowell, J. A., Sigman, C. C., and Kellof, G. J. (1999) Lipoxygenase Inhibitors as Potential Cancer Chemopreventives. *Cancer Epidemiol., Biomarkers Prev. 8*, 467–483.
(6) Hussain, H., Shornick, L. P., Shannon, V. R., Wilson, J. D., Funk, C. D., Pentland, A. P., and Holtzman, M. J. (1994) Epidermis contains platelet-type 12-lipoxygenase that is overexpressed in germinal layer keratinocytes in psoriasis. *Am. J. Physiol. 266*, C243–C253.
(7) Connolly, J. M., and Rose, D. P. (1998) Enhanced angiogenesis and growth of 12-lipoxygenase gene-transfected MCF-7 human breast cancer cells in athymic nude mice. *Cancer Lett. 132*, 107–112.
(8) Natarajan, R., and Nadler, J. (1998) Role of lipoxygenases in breast cancer. *Front. Biosci. 3*, E81–E88.
(9) Harats, D., Shaish, A., George, J., Mulkins, M., Kurihara, H., Levkovitz, H., and Sigal, E. (2000) Overexpression of 15-lipoxygenase in vascular endothelium accelerates early atherosclerosis in LDL receptor-deficient mice. *Arterioscler. Thromb. Vasc. Biol. 20*, 2100–2105.

(10) Kamitani, H., Geller, M., and Eling, T. (1998) Expression of 15-lipoxygenase by human colorectal carcinoma Caco-2 cells during apoptosis and cell differentiation. *J. Biol. Chem. 273*, 21569–21577.
(11) Shappell, S. B., Manning, S., Boeglin, W. E., Guan, Y. F., Roberts, R. L., Davis, L., Olson, S. J., Jack, G. S., Coffey, C. S., Wheeler, T. M., Breyer, M. D., and Brash, A. R. (2001) Alterations in lipoxygenase and cyclooxygenase-2 catalytic activity and mRNA expression in prostate carcinoma. *Neoplasia 3*, 287–303.
(12) Butler, R. M., S. H., Tindall, D. J., and Young, C. Y. (2000) Nonapoptotic cell death associated with S-phase arrest of prostate cancer cells via the peroxisome proliferator-activated receptor gamma ligand, 15-deoxy-Δ12,14-prostaglandin J2. *Cell Growth Differ. 11*, 49–61.
(13) Hsi, L. C., Wilson, L., Nixon, J., and Eling, T. E. (2001) 15-Lipoxygenase-1 metabolites down-regulate peroxisome proliferator-activated receptor γ via the MAPK signaling pathway. *J. Biol. Chem. 276*, 34545–34552.
(14) Wecksler, A. T., Kenyon, V., Deschamps, J. D., and Holman, T. R. (2008) Substrate specificity changes for human reticulocyte and epithelial 15-lipoxygenases reveal allosteric product regulation. *Biochemistry 47*, 7364–7375.
(15) Brash, A. R., Boeglin, W. E., and Chang, M. S. (1997) Discovery of a second 15S-lipoxygenase in humans. *Proc. Natl. Acad. Sci. U.S.A. 94*, 6148–6152.
(16) Kilty, I., Logan, A., and Vickers, P. J. (1999) Differential characteristics of human 15-lipoxygenase isozymes and a novel splice variant of 15S-lipoxygenase. *Eur. J. Biochem. 266*, 83–93.
(17) Ruddat, V. C., Mogul, R., Chorny, I., Chen, C., Perrin, N., Whitman, S., Kenyon, V., Jacobson, M. P., Bernasconi, C. F., and Holman, T. R. (2004) Tryptophan 500 and arginine 707 define product and substrate active site binding in soybean lipoxygenase-1. *Biochemistry 43*, 13063–13071.
(18) Glickman, M. H., and Klinman, J. P. (1996) Lipoxygenase reaction mechanism: Demonstration that hydrogen abstraction from substrate precedes dioxygen binding during catalytic turnover. *Biochemistry 35*, 12882–12892.
(19) Glickman, M. H., and Klinman, J. P. (1995) Nature of rate-limiting steps in the soybean lipoxygenase-1 reaction. *Biochemistry 34*, 14077–14092.
(20) Rickert, K. W., and Klinman, J. P. (1999) Nature of hydrogen transfer in soybean lipoxygenase 1: Separation of primary and secondary isotope effects. *Biochemistry 38*, 12218–12228.
(21) Segraves, E. N., and Holman, T. R. (2003) Kinetic investigations of the rate-limiting step in human 12- and 15-lipoxygenase. *Biochemistry 42*, 5236–5243.
(22) Jacquot, C., Peng, S., and van der Donk, W. A. (2008) Kinetic isotope effects in the oxidation of arachidonic acid by soybean lipoxygenase-1. *Bioorg. Med. Chem. Lett. 18*, 5959–5962.
(23) Jacquot, C., Wecksler, A. T., McGinley, C. M., Segraves, E. N., Holman, T. R., and van der Donk, W. A. (2008) Isotope sensitive branching and kinetic isotope effects in the reaction of deuterated arachidonic acids with human 12- and 15-lipoxygenases. *Biochemistry 47*, 7295–7303.
(24) Lewis, E., Johnson, E., and Holman, T. (1999) Large Competitive Kinetic Isotope Effects in Human 15-Lipoxygenase Catalysis Measured by a Novel HPLC Method. *J. Am. Chem. Soc. 121*, 1395–1396.
(25) Peng, S., Okeley, N. M., Tsai, A. L., Wu, G., Kulmacz, R. J., and van der Donk, W. A. (2002) Synthesis of isotopically labeled arachidonic acids to probe the reaction mechanism of prostaglandin H synthase. *J. Am. Chem. Soc. 124*, 10785–10796.
(26) Peng, S., McGinley, C. M., and van der Donk, W. A. (2004) Synthesis of site-specifically labeled arachidonic acids as mechanistic probes for prostaglandin H synthase. *Org. Lett. 6*, 349–352.
(27) Amagata, T., Whitman, S., Johnson, T. A., Stessman, C. C., Loo, C. P., Lobkovsky, E., Clardy, J., Crews, P., and Holman, T. R. (2003) Exploring sponge-derived terpenoids for their potency and selectivity against 12-human, 15-human, and 15-soybean lipoxygenases. *J. Nat. Prod. 66*, 230–235.
(28) Chen, X. S., Brash, A. R., and Funk, C. D. (1993) Purification and characterization of recombinant histidine-tagged human platelet 12-lipoxygenase expressed in a baculovirus/insect cell system. *Eur. J. Biochem. 214*, 845–852.
(29) Deems, R., Buczynski, M. W., Bowers-Gentry, R., Harkewicz, R., and Dennis, E. A. (2007) Detection and Quantitation of Eicosanoids via High Performance Liquid Chromatography-Electrospray Ionization-Mass Spectrometry. *Methods Enzymol. 432*, 59–82.
(30) Knapp, M. J., and Klinman, J. P. (2003) Kinetic studies of oxygen reactivity in soybean lipoxygenase-1. *Biochemistry 42*, 11466–11475.
(31) Knapp, M. J., Rickert, K., and Klinman, J. P. (2002) Temperature-dependent isotope effects in soybean lipoxygenase-1: Correlating hydrogen tunneling with protein dynamics. *J. Am. Chem. Soc. 124*, 3865–3874.
(32) Basran, J., Patel, S., Sutcliffe, M. J., and Scrutton, N. S. (2001) Importance of barrier shape in enzyme-catalyzed reactions. Vibrationally assisted hydrogen tunneling in tryptophan tryptophylquinone-dependent amine dehydrogenases. *J. Biol. Chem. 276*, 6234–6242.
(33) Masgrau, L., Basran, J., Hothi, P., Sutcliffe, M. J., and Scrutton, N. S. (2004) Hydrogen tunneling in quinoproteins. *Arch. Biochem. Biophys. 428*, 41–51.
(34) Edwards, S. J., Soudackov, A. V., and Hammes-Schiffer, S. (2009) Analysis of Kinetic Isotope Effects for Proton-Coupled Electron Transfer Reactions. *J. Phys. Chem. A 113*, 2117–2126.
(35) Kiefer, P. M., and Hynes, J. T. (2004) Kinetic Isotope Effects for Nonadiabatic Proton Transfer Reactions in a Polar Environment. 1. Interpretation of Tunneling Kinetic Isotopic Effects. *J. Phys. Chem. A 108*, 11793–11808.
(36) Cukier, R. I. (2002) A Theory that Connects Proton-Coupled Electron-Transfer and Hydrogen-Atom Transfer Reactions. *J. Phys. Chem. B 106*, 1746–1757.
(37) Bell, R. P. (1980) The Tunneling Effects in Chemistry , Chapman and Hall, London.
(38) Melander, L. S. (1987) Reaction Rates of Isotopic Molecules , R. E. Krieger, Malabar, FL.
(39) Kuhn, H. (2000) Structural basis for the positional specificity of lipoxygenases. *Prostaglandins Other Lipid Mediators 62*, 255–270.
(40) Peng, S., and van der Donk, W. A. (2003) An unusual isotope effect on substrate inhibition in the oxidation of arachidonic acid by lipoxygenase. *J. Am. Chem. Soc. 125*, 8988–8989.
(41) Hudetz, A. G. (1999) Mathematical model of oxygen transport in the cerebral cortex. *Brain Res. 817*, 75–83.
(42) Parker, C., Milosevic, M., Toi, A., Sweet, J., Panzarella, T., Bristow, R., Catton, C., Catton, P., Crook, J., Gospodarowicz, M., McLean, M., Warde, P., and Hill, R. P. (2004) Polarographic electrode study of tumor oxygenation in clinically localized prostate cancer. *Int. J. Radiat. Oncol., Biol., Phys. 58*, 750–757.
(43) Saam, J., Ivanov, I., Walther, M., Holzhutter, H. G., and Kuhn, H. (2007) Molecular dioxygen enters the active site of 12/15-lipoxygenase via dynamic oxygen access channels. *Proc. Natl. Acad. Sci. U.S.A. 104*, 13319–13324.